RSC Applied Polymers

ROYAL SOCIETY OF CHEMISTRY

PAPER

View Article Online
View Journal | View Issue

Cite this: *RSC Appl. Polym.*, 2025, **3**, 662

Functional self-healing aldehyde-derived nanoparticle-crosslinked gelatin/PNIPAm-based adhesive gels†

P. A. Parvathy,[a,b] Sriparna De,[c] Manjinder Singh,[d] Gaurav Manik [d] and Sushanta K. Sahoo*[a,b]

The combination of lower critical solution temperature (LCST) and upper critical solution temperature (UCST) polymers provides varying dissolution to the system, with tunable physiochemical properties. In the current work, injectable, fluorescent, and thermo-responsive poly-*N*-isopropylacrylamide (PNIPAm)-gelatin nanocomposite gels were prepared by combining non-covalent interactions and Schiff base chemistry. The incorporation of aldehyde-based nanoparticles (2.5–10%) facilitated the crosslinking of the matrix *via* the formation of imine linkages with gelatin, which significantly reduced the pore size of the gels from 30–40 micron to 4–5 μm. The temperature-dependent viscoelastic properties showed that the storage modulus increased significantly above 40 °C, which confirmed the thermosensitive behaviour of the gels owing to the combined effect of PNIPAm and gelatin. Higher storage modulus over loss modulus for all crosslinked gels indicates the elastic behaviour of the gels. The introduction of imine linkages offered instant self-healing features and the nanoparticles provide photoluminescence to the polymeric gel system. Furthermore, the tackiness offered by gelatin enhances the adherence to human skin and the gels are found to be biocompatible towards fibroblast cell lines (L929) and are promising for drug delivery systems, injectable materials, and optically trackable adhesives. The findings provide new insights into the multifunctional properties of thermoresponsive PNIPAm-gelatin nanocomposite gels with dynamic imine linkages for biological applications.

Received 12th February 2025,
Accepted 4th March 2025

DOI: 10.1039/d5lp00038f

rsc.li/rscapplpolym

1. Introduction

Injectable, self-healing, responsive gels encompass dynamic and reversible three-dimensional network architectures capable of reinstating their original structure and functionality after damage.[1,2] They have garnered significant attention due to their favourable properties, such as bio-compatibility, simple formation, ease of handling, adaptability.[3–5] Additionally, they have emerged as versatile intelligent materials for biomedical applications, including drug delivery,[6] regenerative medicine,[1] and tissue engineering.[7] The chemical strategies to prepare self-healing hydrogels involve the introduction of either non-covalent interactions, dynamic covalent interactions or a combination of both. Non-covalent interactions include electrostatic interactions,[8] metal coordination,[9] hydrophobic interactions[10] and hydrogen bonding,[11] whereas dynamic covalent interactions include the introduction of imine bonds (Schiff base),[12] disulfide linkages,[13] Diels–Alder reaction,[14] boronate ester,[15] and acyl hydrazone.[16] Among these, imine bonds are considered more stable in various media, such as solvent, hydrolytic, alkaline and neutral media, and they are recyclable.[17–21]

Nano-crosslinked hydrogels contain dynamic interactions, integrating the inherent characteristics of nanoparticles as well as demonstrating the distinct benefits of the matrix components through dynamic bonds.[22] The incorporation of nanoparticles as crosslinkers enhances the strength and injectability of the hydrogels by fortifying the structure, and also imparts multi-functionality, such as response to external stimuli (pH, temperature, and light), anti-bacterial and anti-oxidant properties.[23–25] Nanomaterials possess highly specific surfaces that facilitate physical and chemical interaction with polymers and exhibit unique nanoscale characteristics for medicinal applications, including drug administration,

[a]*Materials Science and Technology Division, CSIR-National Institute for Interdisciplinary Science and Technology, Thiruvananthapuram 695019, India. E-mail: sushanta@niist.res.in*
[b]*Academy of Scientific and Innovative Research (AcSIR), Ghaziabad-201002, India*
[c]*Department of Allied Health Sciences, Brainware University, Kolkata 700125, India*
[d]*Department of Polymer and Process Engineering, Indian Institute of Technology, Roorkee 247667, India*

† Electronic supplementary information (ESI) available. See DOI: https://doi.org/10.1039/d5lp00038f

tumour therapy, and tissue regeneration.[22] The nanomaterials used in dynamic hydrogel fabrication include metals and metallic oxides,[26] nanoclays,[27] carbon-based nanomaterials,[28] black phosphorus,[29] and polymeric nanomaterials.[30] Furthermore, the fluorescent properties of nanomaterials helps to provide optical tracing characteristics to the gel system.

A variety of polymeric materials have been used as structural components in the development of self-healing injectable gels. Natural polymers often used in such gels include gelatin, collagen, hyaluronic acid, alginate, and chitosan, due to their features such as inherent biomedical qualities, ease of availability, and biocompatibility.[31,32] Gelatin is a UCST-type polymer, which exhibits a gel nature below the UCST (40 °C) and a liquid nature above the UCST[33–36] (hydrophobic to hydrophilic transition). Collagen-derived gelatin has exceptional biocompatibility and is used in several biomedical applications.[37] Thus, gelatin has been reported to be miscible with other polymers to achieve optimal gelling characteristics and maintain stability at physiological temperatures.[38] The thermo-responsive properties of gelatin have been investigated for drug delivery systems.[35,36] NIPAm is a prominent thermo-responsive polymer that has a LCST of 32 °C, which is near the physiological temperature. The ability to adjust the LCST up to the desired value and modify the structure with various synthetic or bio-based monomers/polymers enhances the demand for PNIPAm-based materials. PNIPAm-based hydrogels are extensively investigated as biomedical and smart materials, such as drug delivery systems, wound healing materials, and cell culturing systems.[39–43] The combination of a LCST and UCST polymer, known as a "schizophrenic polymer[44]", a type of dual thermo-responsive polymer with complex dissolution behaviour, helps in applications such as drug delivery and theranostics.[45]

Aggarwal *et al.* prepared fluorescent self-healing injectable hydrogels from gelatin, cross-linked *via* Schiff base chemistry using dopamine-terephthaldehyde (TA)-based carbon dots. The gels were biocompatible (>90%) and exhibited antibacterial activity towards *E. coli* and *S. aureus*.[46] Sun *et al.* synthesised self-healing hydrogels from gallic acid coupled with P(NIPAm-*co*-AH) and oxidised sodium alginate. An amine-modified PNIPAm copolymer served as a crosslinking point *via* Schiff base reaction and the gels showed adhesive properties to different substrates (rubber, metal, heart, spleen, *etc.*).[47] Khodaei *et al.* prepared self-healing hydrogels from aldehyde-modified carrageenan and dopamine using Schiff base chemistry, and the gel was found to possess a better storage modulus of 800 Pa and a shear thinning effect.[48]

The aim of this work is to develop thermo-responsive self-healable-fluorescent bio-adhesive gels through the integration of a LCST polymer (PNIPAm), a UCST polymer (gelatin) and aldehyde-grafted carbon-based nanoparticles, while cross-linking through the formation of reversible imine bonds. The gel system integrates physical (hydrogen bonding) and dynamic covalent interactions through Schiff base chemistry utilizing TA-based nanoparticles (TNs) with gelatin, which has not been reported so far. The formation of the –C═N chromophore through the conjugation of nanoparticles imparts self-healing, intrinsic photoluminescence properties, and tunable pore size, endowing it with potential as a bio-adhesive to trace and monitor the affected skin or wounds. The conjugation of fluorescent TN augmented the photoluminescence (PL) intensity of the gels, which is essential for optical tracing.

2. Experimental

2.1 Materials

NIPAm (97.0%) and gelatin were procured from Sigma Aldrich. Azobisisobutyronitrile (AIBN) (98.0%) was purchased from Himedia and TA (>98.0%) was obtained from TCI chemicals. The solvent methanol was obtained from Merck (99.5%) and absolute ethanol from Analytical CSS reagents. The chemicals were used without further purification. Mouse fibroblast cells (L929) were procured from the National Centre for Cell Science (NCCS, 36 Pune, India), along with the cell culture media. Fetal bovine serum (FBS), and Dulbecco's modified Eagle's 40 medium (DMEM) (99%) were obtained from Himedia and MTT reagent (97.5%) was procured from Sigma Aldrich.

2.2 Preparation of the PNIPAm-gelatin polymer system (P5G5)

NIPAm (1 g) and AIBN (0.014 g) were mixed into a 1 wt% gelatin solution (100 mL, solvent combination of methanol : water = 1 : 9) under a nitrogen environment at room temperature for 48 h to get the polymeric solution (Scheme 1).[49] Different ratios of NIPAm : gelatin were employed to prepare the polymeric solution as depicted in Table 1. Based on its

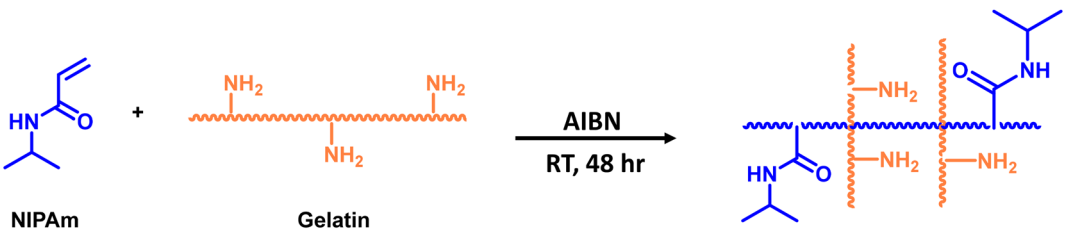

Scheme 1 Synthetic procedure of the PNIPAm-gelatin polymeric solution.

Table 1 Composition of PNIPAm-gelatin

Sample	NIPAm (%)	Gelatin (%)
P4G6	40	60
P5G5	50	50
P6G4	60	40

Table 2 Composition of the nano-crosslinked gels

Sample	TN (wt%)
P5G5-TN 2.5	2.5
P5G5-TN 5	5
P5G5-TN 7.5	7.5
P5G5-TN 10	10

better miscibility, P5G5 was selected for preparing the solution and then concentrated to one fourth of the initial volume by removing solvent for the next step.

2.3 Synthesis of the PNIPAm-gelatin nanocomposite gels

The nanocomposite gels were prepared *via* a two-step process (Scheme 2). TA-based nanoparticles were synthesized by employing a solvothermal process. 0.2 g of TA was dissolved in 40 mL methanol and autoclaved at 180 °C for 12 h. The yellow colour solution obtained after the process was filtered using a syringe filter (0.22 μm), and the solvent was evaporated to get TN nanoparticles in powder form. Nanocomposite hydrogels were synthesized *via* mixing the polymeric solutions with different weight percentages of TN nanoparticles dissolved in ethanol (Table 2). The pH of the solution was adjusted to 8 and the reaction was proceeded at 70 °C for 24 h. The obtained yellow gel was subjected to further characterization.

2.4 Characterization

TA and TN nanoparticles were characterised using FT-IR [ATR-FT-IR spectrophotometer (PerkinElmer)] in the range of 4000 cm^{-1} to 400 cm^{-1} and ^{1}H-NMR [500 MHz Bruker Avance DPX spectrometer using acetone-d_6 as a solvent]. UV-Vis analysis of the TA and TN solutions and crosslinked gels was conducted using a UV-2700i UV-vis spectrophotometer (Shimadzu) and photoluminescence (solution) was studied using a Yvon Fluorolog 3 spectrofluorimeter using a 450 W xenon flash lamp as the excitation source. The particle size of the TN was measured with a ZetaPals DLS/zeta potential analyser (0.5 mg ml^{-1} in acetone). Furthermore, the particle size of the TN was determined using high-resolution transmission electron microscopy (FEI, Tecnai G2, T30 S-TWIN).

The polymerization of PNIPAm and its interaction with gelatin and crosslinking were confirmed with FT-IR-ATR analysis of NIPAm, gelatin and the crosslinked gels. X-ray diffraction analysis was performed under Cu Kα radiation in a Malvern Panalytical diffractometer at a diffraction angle (2θ) of 10° and 90°, respectively. SEM (Carl Zeiss EVO MA18 FE SEM) was used to analyse the morphology of the freeze-dried gels, which are operating at an accelerating voltage of 15 kV. Differential scanning calorimetry (DSC) of the cross-linked gels in water was performed using a Discovery series DSC 25, TA instrument at a heating rate of 2 °C min^{-1} under a N_2 atmosphere. The temperature-dependent viscoelastic properties of the polymer and crosslinked gels were studied using a Rheometer (MCR102, ANTONPAAR, USA), in the temperature range of 25–60 °C. The images of the gels and TA and TN solutions under UV were taken using a SPECTROLINE Model CM-10A fluorescence analysis cabinet (365 nm illumination). Adhesion of the gels was tested using different substrates, such as metal, plastic, glass and skin.

2.5 MTT assay

The National Centre for Cell Science (NCCS) in Pune, India, provided the mouse L929 fibroblast cells utilized in this study to evaluate cell growth and survival on the composites. The cells were grown in DMEM, given synthetic formulations, and their cytotoxicity was monitored. *In vitro* cytotoxicity was investigated using the MTT assay.[50] Each well's optical density (OD)

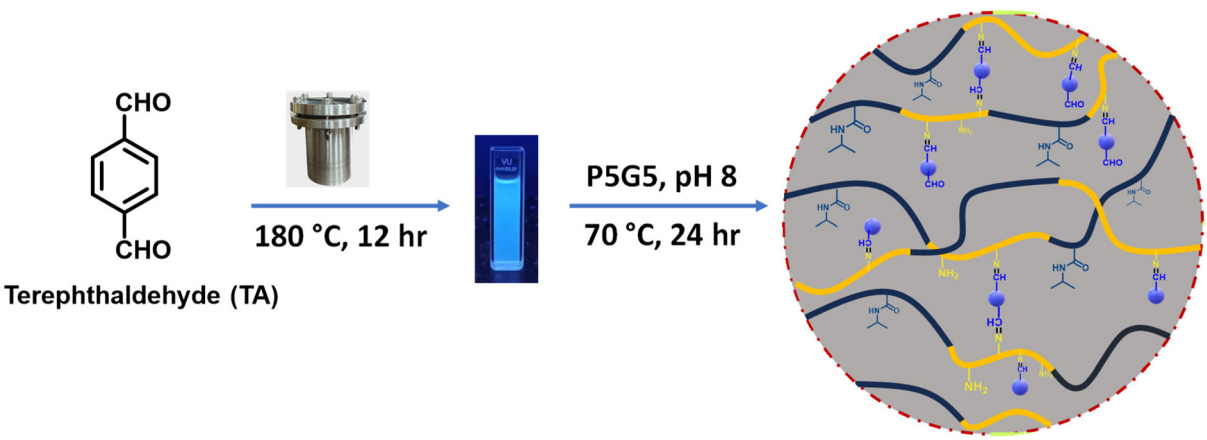

Scheme 2 Preparation the PNIPAm-gelatin-TN nanocomposite gels.

was measured, and the following formula was used to assess the relative cell viability:

$$\%\,\text{cell viability} = \frac{\text{OD}_{\text{sample}} - \text{OD}_{\text{control}}}{\text{OD}_{\text{control}}} \times 100$$

To examine the effect of the materials on cell growth, the investigation was conducted in triplicate.

3. Results and discussion

3.1 TA nanoparticle characteristics

TA was chosen as the organic compound for preparing the nanoparticles, which can cross-link with the $-NH_2$ groups of gelatin through Schiff base chemistry.[46,51] The FT-IR-ATR spectra shown in Fig. 1a verified the retention of the aldehyde peak of TA in the TNs at 1682 cm^{-1} after the solvothermal process. The signal associated with the aldehydic proton in the TNs presented at 10 ppm in the ^1H NMR (Fig. 1b). DLS analysis yields the hydrodynamic diameter of the TN particles at around 160 nm (Fig. 1c). The size for nanoparticle aggregation was further validated using TEM imaging (Fig. 1d). The particle dimensions were determined to be between 60 and 70 nm at the aggregation corners. The aggregation of the particles can be attributed to hydrogen bond interactions between the aldehyde groups and π–π stacking. The particle sizes seen in DLS data are often augmented due to the solvent's impact. A comparison of the XRD patterns is shown in the ESI (Fig. S1†), indicating that the degree of modification in the TNs relative to TA is minimal.

Fig. 2a and b illustrate the absorbance and photoluminescence spectra of the nanoparticles. The broad absorption peak seen at 330 nm is attributed to the n–π* transition in the TNs (Fig. 2a).[52] The peak intensity and broadness increased compared to TA, owing to the development of discrete energy levels during the solvothermal process. PL ana-

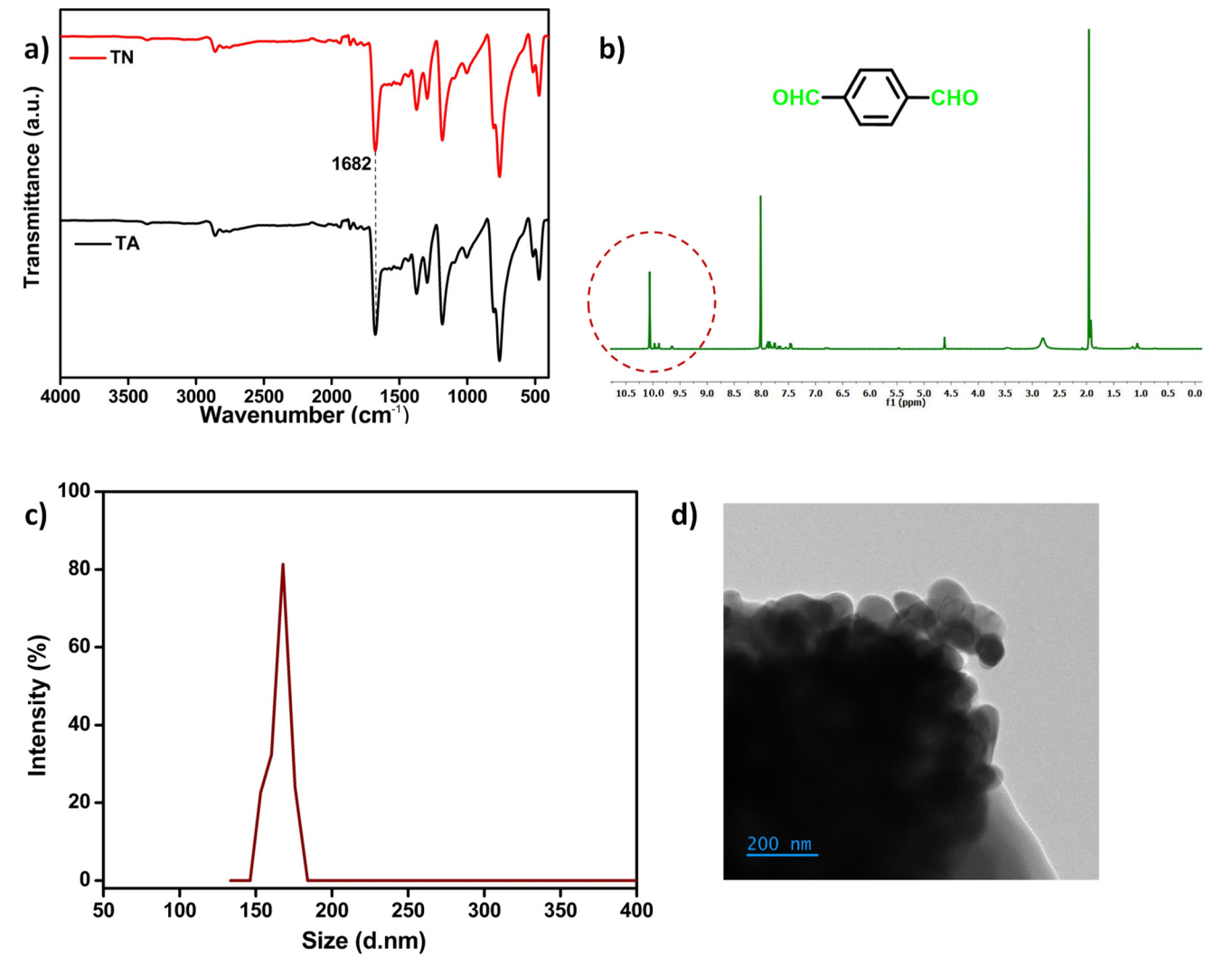

Fig. 1 (a) FT-IR-ATR comparison of TA and the TNs, (b) ^1H NMR spectra of the TNs in acetone-d_6, (c) DLS spectra of the TNs in acetone (0.5 mg ml^{-1}) and (d) TEM image of the TN particles.

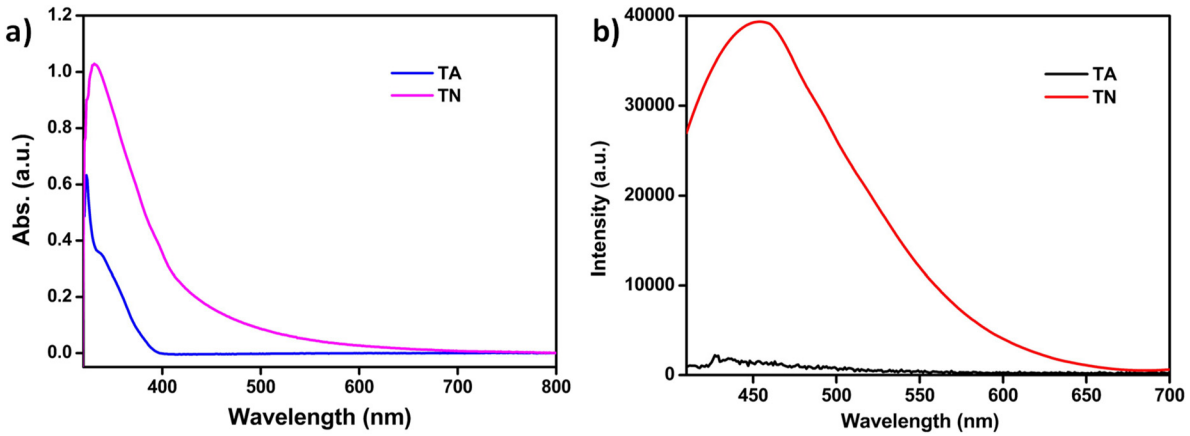

Fig. 2 (a) UV-Vis and (b) PL spectra of the TNs in acetone.

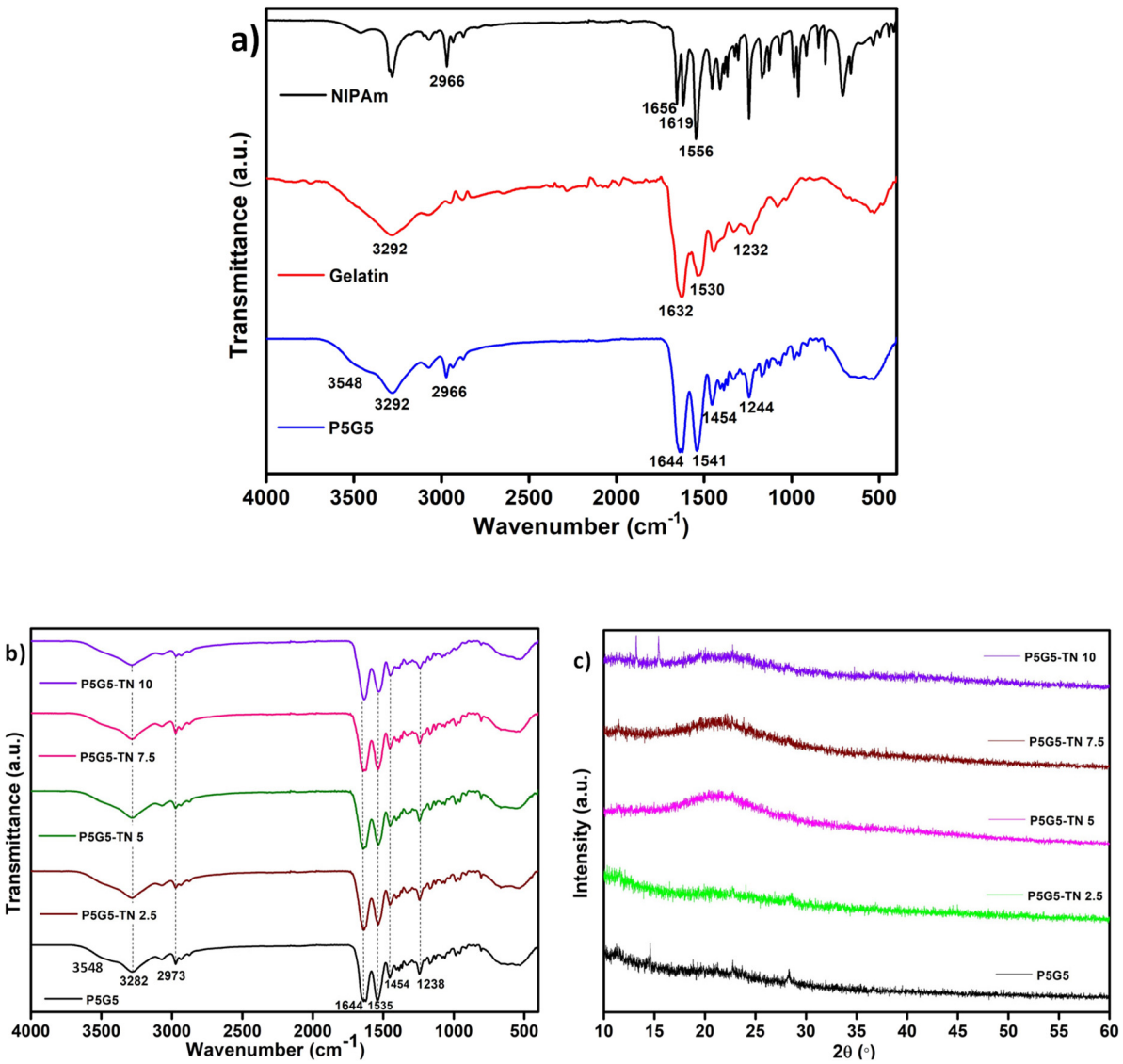

Fig. 3 (a) FT-IR-ATR analysis of the NIPAm, gelatin, and P5G5 and (b) crosslinked gels, and (c) the XRD pattern comparison.

lysis confirmed the fluorescent behaviour of the nanoparticles. The emission spectra (exc. 380 nm) can be correlate with UV analysis, where the intensity of the TN solution changed significantly compared to TA (Fig. 2b). An image depicting a comparison of the TN and TA solutions under UV light is given in the ESI (Fig. S2†).

3.2 PNIPAm-gelatin nanocomposite gel

Radical polymerization was used to synthesize the PNIPAm polymer using AIBN as the initiator, in which gelatin was introduced to interact with the polymer through physical means. Furthermore, the gels were synthesized by Schiff-base chemistry involving the –CHO groups of TN and the –NH_2 groups of

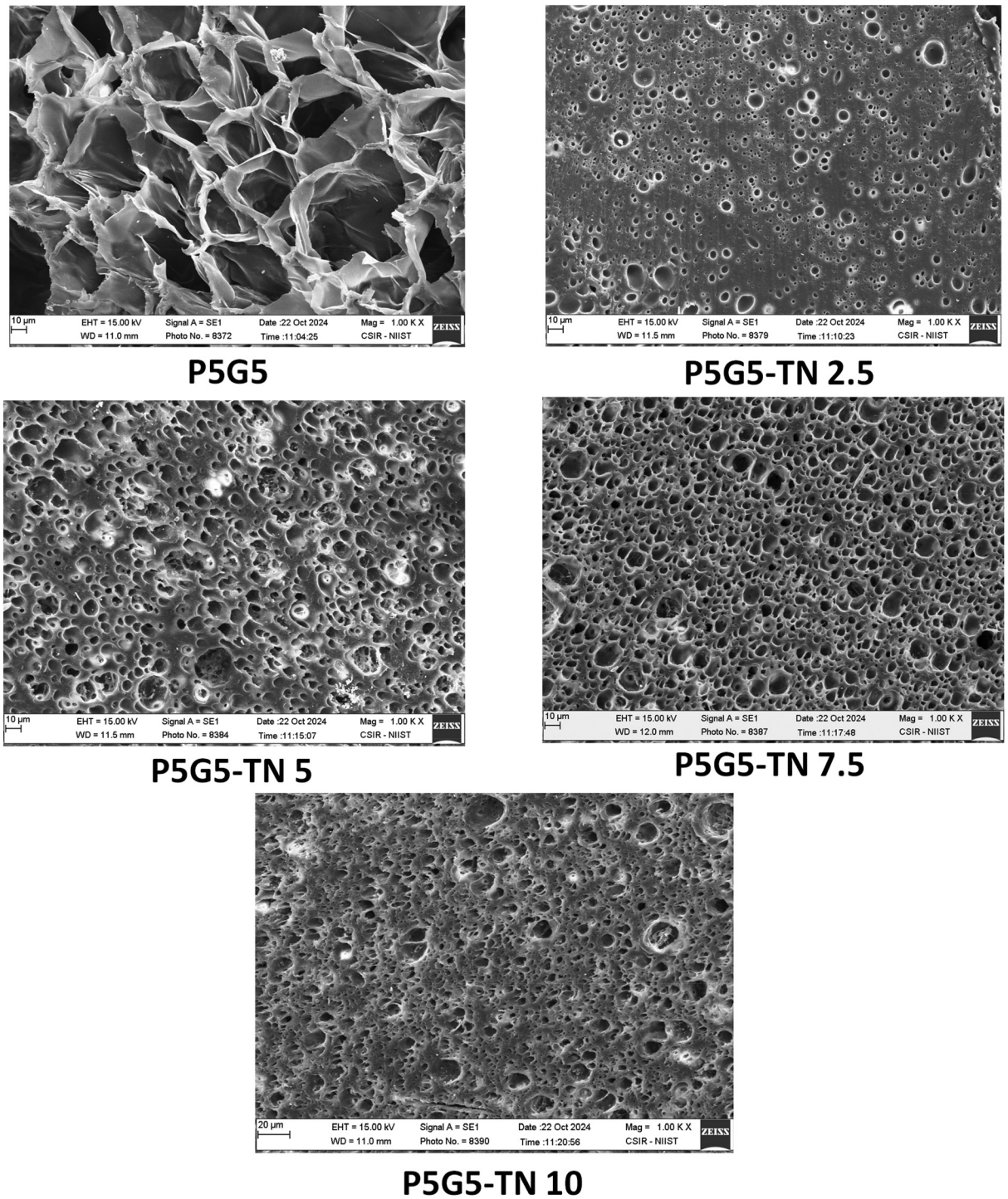

Fig. 4 Morphology of the freeze-dried gels.

gelatin. Under acidic pH conditions, the crosslinking reaction between the –CHO and –NH_2 functional groups results in the formation of hemiacetals, while in alkali medium, the reaction predominantly involves the formation of Schiff bases.[53] Here, the preparation of P(NIPAm-gelatin)-TN was conducted at pH 8 and the polymeric solution transitioned to a sticky gel after crosslinking, along with a change from transparent to a yellow hue. FT-IR analysis was conducted to confirm the polymerization and crosslinking (Fig. 3a and b). In the FT-IR data of P5G5 (Fig. 3a), the broader absorption band around 3548 cm^{-1} indicates hydrogen bond formation between the –OH and –NHCO groups. Moreover, the bands usually occurring at 1656 cm^{-1} and 1556 cm^{-1} in the spectrum of NIPAm shifted to 1644 cm^{-1} and 1541 cm^{-1}, respectively, indicating hydrogen bonding interactions between gelatin and PNIPAm.[49,54] The peak corresponding to C=C at 1619 cm^{-1} in NIPAm got reduced in P5G5 confirming the polymerization.[49] The hydrogen bonding between NIPAm and gelatin enables the polymeric solution to be highly miscible. The Schiff base formation was confirmed *via* conducting the reaction of TNs with gelatin and the corresponding FT-IR-ATR analysis is depicted in Fig. S3.† The aldehydic peak (1682 cm^{-1}) arising from the TNs completely disappeared in the gelatin-TN system. The amide I and amide II bands, located at approximately 1632 and 1530 cm^{-1}, respectively, are typical spectral features for gelatin. Since the peak for imine –C=N– stretching vibration lies in the range of 1640–1690 cm^{-1}, it overlaps with the strong band for amide I in gelatin. These results are consistent with those of Joy *et al.*,[55] Qian *et al.*[56] and Dong *et al.*[57] A similar fact was observed in the case of the crosslinked gels. No aldehydic peak was observed in the nanocomposite gels. TN doesn't alter the peak positions except that it reduces the broadness of the peak for amide at 1530 cm^{-1} and the peak at 3548 cm^{-1}. The XRD pattern of the gels depicted in Fig. 3c clarifies the amorphous nature of the gels. The nanoparticles effectively crosslinked with the gelatin system and the presence of sharp peaks in P5G5-TN10 indicates a surplus amount of TNs that could not take part in crosslinking.

3.2.1 SEM analysis. The morphology of the composition P5G5 and the gels in the freeze-dried state is shown in the Fig. 4. The 3D microporous morphology shows a significant decrease in porosity of the P5G5-TN nanocomposite compared to P5G5. The pore diameter measured around 35 to 40 μm is significantly reduced to 4–5 μm in the nanocomposite gels.

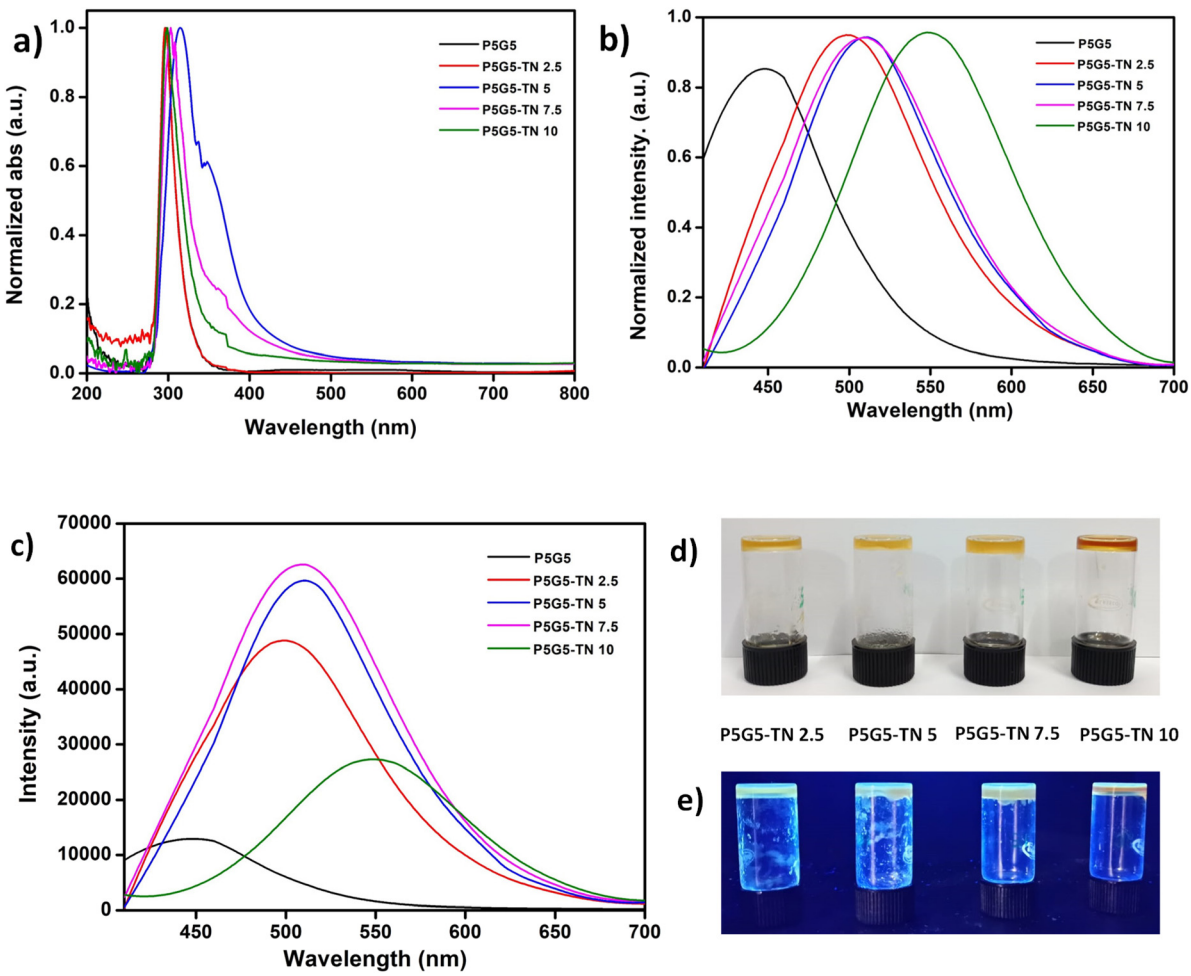

Fig. 5 (a) UV-Vis and (b) and (c) PL spectra of the P5G5 and nanocomposite gels, and images of the gels under (d) visible and (e) UV light.

The reduction in pore size can serve as direct evidence of crosslinking *via* Schiff-base reaction. The presence of smaller pores is beneficial to transfer the load throughout the structure.[58] Gels with a microporous structure can incorporate lower molecular sized drugs for drug delivery applications. Additionally, it can help with nutrient transport, waste removal, cell growth *etc.*[59]

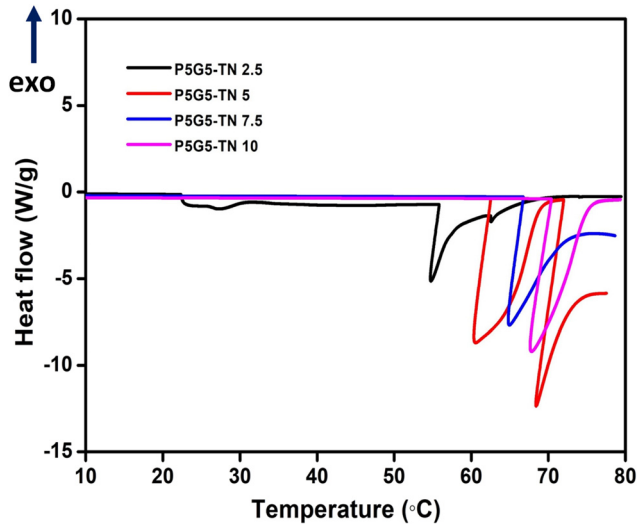

Fig. 6 DSC thermogram of the nanocomposite hydrogels.

3.2.2 Photophysical features. The UV-Vis spectrum of P5G5 and the nanocomposite gels showed absorption maxima in the range of 297–314 nm, which can be attributed to the major n–π* transition (Fig. 5a). The occurrence of a shoulder peak in the composite at 365 nm corresponds to the chromophore –C═N formed as a result of Schiff base reaction. The photoluminescence spectrum shows a red shift of the peak maxima in the nanocomposite gels (450 to 549 nm, ext. 380 nm) compared to P5G5, which further confirms the presence of an imine bond (Fig. 5b). Similar results were observed by Aggarwal *et al.*,[46] where imine bonds caused a red shift in gelatin/CD composite hydrogels. The intensity of the spectrum of the gels continuously increased until 7.5 wt% TNs (P5G5-TN 7.5) and got reduced in P5G5-TN 10 (Fig. 5c). The sudden drop in intensity may be due to the aggregation of excess TN in the system and these results can be correlated with the XRD spectra and TEM image. The nanocomposite gel appeared brownish yellow in colour (a characteristic of –C═N chromophoric moieties[60]) in vis-light and turned to fluorescent with UV 365 nm illumination (Fig. 5d and e).

3.2.3 DSC analysis. Fig. 6 illustrates the DSC thermogram of the nanocomposite gels. The DSC curve of P5G5 (Fig S4†) exhibits multiple peaks. In the nanocomposite gels, LCST (26–32 °C) corresponding to NIPAm was noticeable only in the

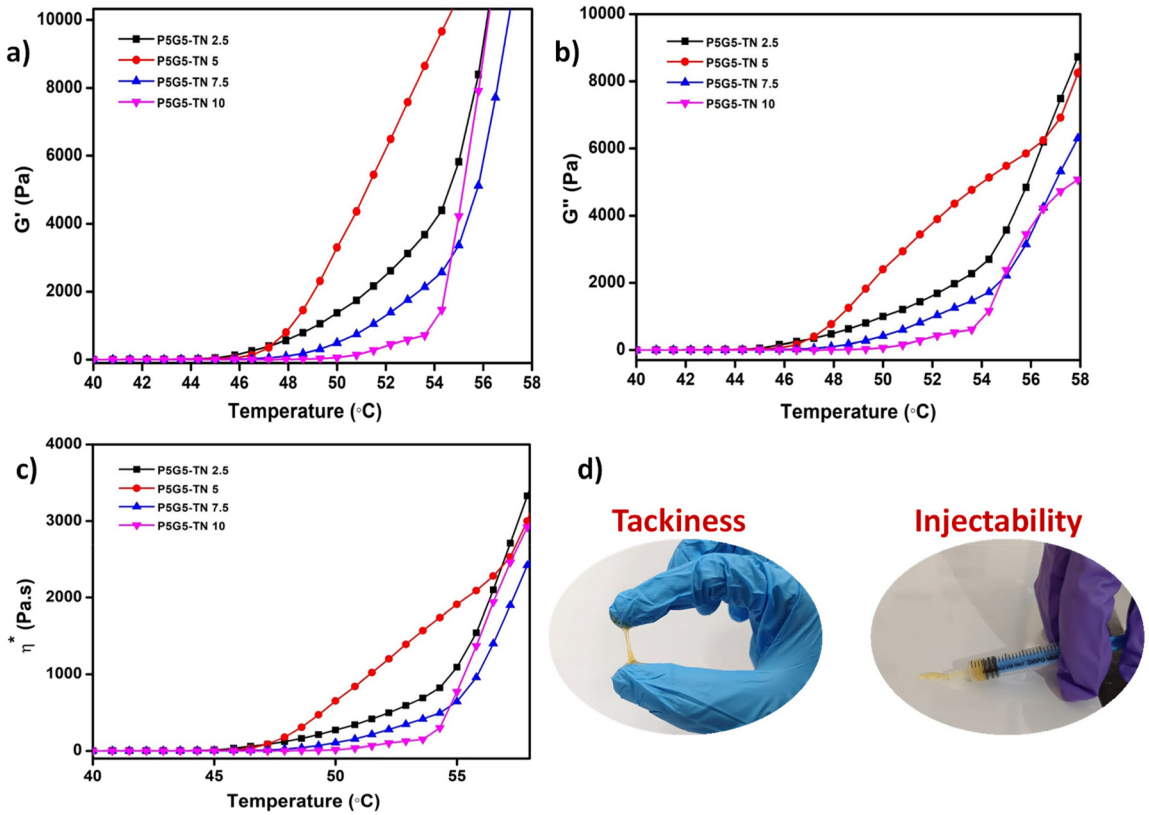

Fig. 7 (a) Storage modulus (*G'*), (b) loss modulus and (c) complex viscosity (*η**) analysis of the nanocomposite gels, and (d) tackiness and injectability.

system (P5G5-TN 2.5) with 2.5% TN content. The mentioned transition disappeared with an increase in TN content above 2.5%. This may be explained due to the effective crosslinking of gelatin, which dominates over the PNIPAM transition. Furthermore, the crosslinked gelatin might have restricted the conformation in the PNIPAm chain owing to supramolecular interactions. The denaturation temperature of gelatin was observed with a broad transition in the range of 45–75 °C in its uncrosslinked state (Fig. S4†). In contrast, in the crosslinked state, this temperature range was narrowed down to a precise value. The value of the denaturation temperature increased with an increase in the extent of cross-linking. This fact is well supported by the two endothermic peaks observed in the case of lower TN content, possibly due to incomplete crosslinking reaction.[61]

3.2.4 Rheology studies and self-healing properties. The viscoelastic properties (storage modulus (G'), loss modulus (G'') and complex viscosity (η^*)) of the polymer and gels were investigated as a function of temperature as shown in Fig. 7 and Fig. S5.† The PNIPAm-gelatin system (uncrosslinked P5G5) displays (Fig. S5†) two distinct modulus curves representing the temperature response of the system, where G' starts to build up at 30 °C corresponding to the LCST behaviour of PNIPAm, which reduces to zero modulus around 40 °C showing the UCST behaviour of gelatin. In the case of the nanocomposite P5G5-TN gels, they exhibit low G', G'' and η^* values at low temperature (below the LCST, which is characteristics of the liquid state). The dissolution of the polymers below the LCST happens due to their dominant hydrophilic nature, resulting in low moduli and viscosity values. PNIPAm starts to coil up above the LCST,[58,62] which causes build-up of the modulus and an increase in the viscosity values around 45–54 °C in the gels. This single transition in the modulus curve symbolises the solid-like behaviour of the gels as noticed in other PNIPAm systems. In addition, the shift in LCST to a higher value may be ascribed to the combined effect of PNIPAm and crosslinked gelatin. Supramolecular interactions and imine bonds formed during crosslinking have a significant influence on the mechanical features of the gels. The nature of the curve and transition are attributed to the com-

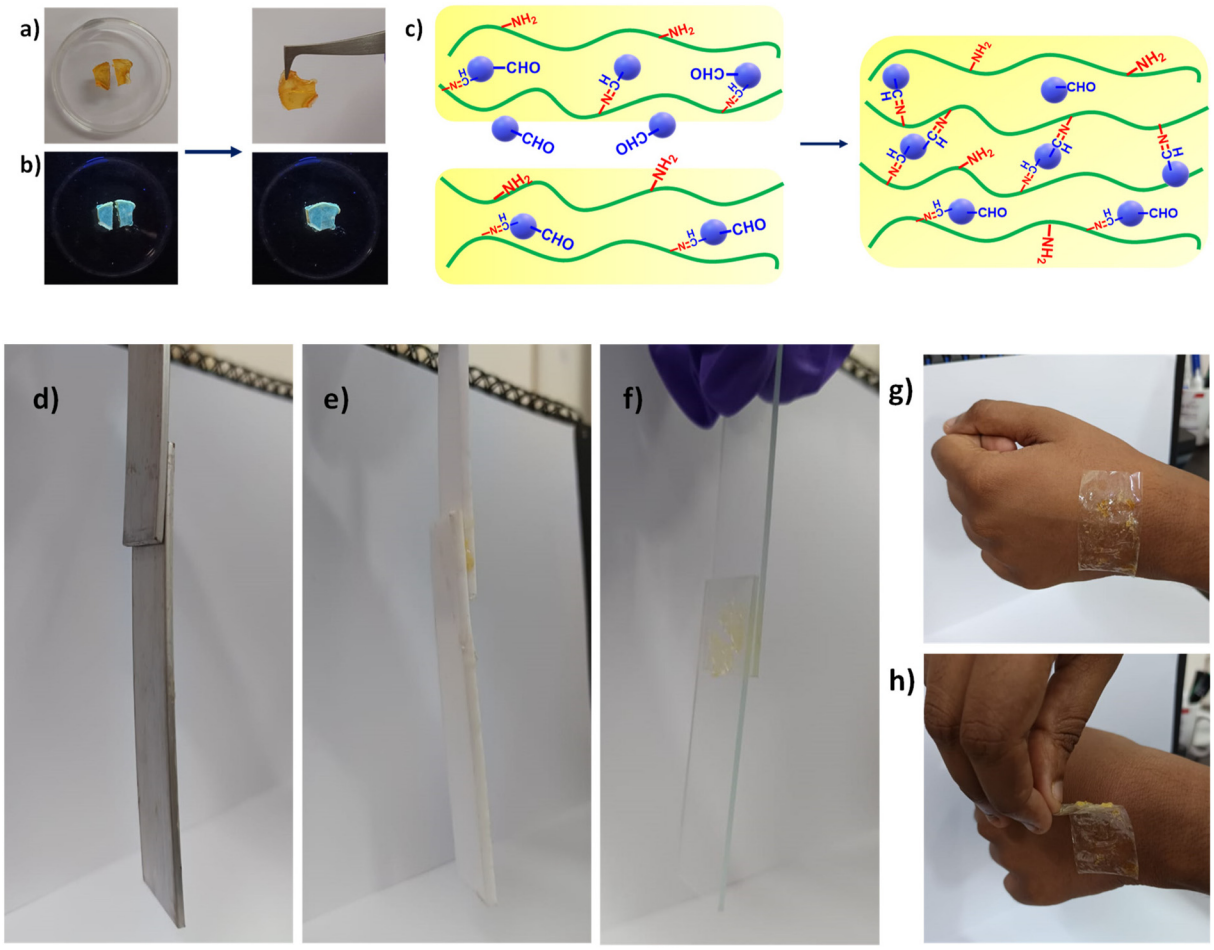

Fig. 8 (a) Self-healing (under visible light) and (b) self-healing (under UV light), and (c) the mechanism behind the self-healing. (d)–(f) Adhesion of the gels to various substrates and (g) and (h) adhesion to skin.

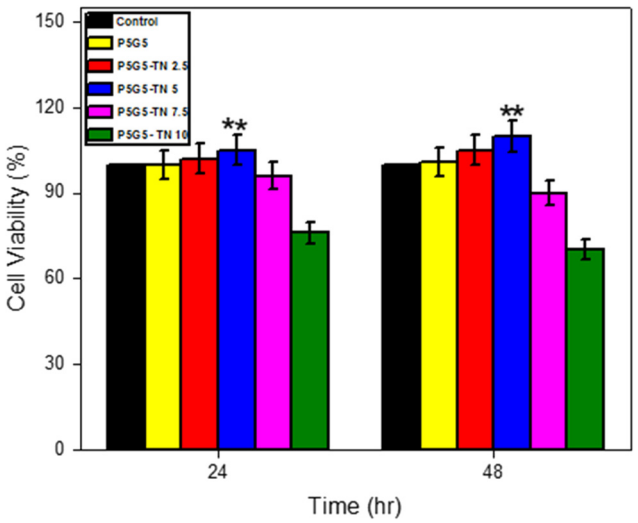

Fig. 9 Cytotoxicity assessment of the fabricated composites and optical micrographs of the *in vitro* cytotoxicity assessment of fibroblast cells (L929) after incubating with different compositions.

bined effect of crosslinked gelatin and the inherent transition of PNIPAm. The presence of amine and aldehyde groups gives tackiness and injectability to the gel (Fig. 7d).

Imines are a class of dynamic covalent bonds that break and repair by themselves. This ability makes the gels self-healable instantly (Fig. 8a and b), for which the mechanism is depicted in Fig. 8c. The adhesion of the gels to different substrates, such as metal, plastic and glass, is depicted in Fig. 8d–f. Fig. 8g and h illustrate the adhesion of gels to the skin, from which they may be easily removed, facilitating their use in bandages.

3.2.5 Biocompatibility analysis. To comprehend the biocompatibility assessment, an MTT assay was performed that correlates with cell viability, making it a useful tool for assessing the cytotoxicity of nanocomposites *in vitro*. Nanocomposites may display time-dependent cytotoxicity, where prolonged exposure to nanomaterials results in apparent cell damage.[62,63] The MTT assay findings demonstrate that the fibroblast cells adequately multiplied and there was no such prominent toxicity profile observed during treatment. Between the control cells and the cells treated with exudates from the P5G5 and terephthaldehyde (TN)-based modified nanocomposites, there was no noticeable change. Importantly, the P5G5-TN5 composites revealed significant cell viability of about ~98.5% in both 24 h and 48 h time intervals, suggesting a comprehensive biocompatibility impact on cell viability and function, enabling better evaluation of its potential for biomedical applications (Fig. 9).[51,64]

4. Conclusions

We developed thermo-responsive nanocomposite gels by utilizing the PNIPAm-gelatin system and crosslinking the amine groups of gelatin with terephthaldehyde nanoparticles *via* Schiff base reaction. The physiochemical properties of the gels stem from the temperature response of PNIPAm and gelatin, together with the dynamic covalent imine bonds produced during the Schiff-base reaction. The gels exhibit fluorescence imparted by TN, injectability, adhesiveness and self-healing properties provided by the imine linkages. The elevated transition in moduli (G' and G'') and viscosity curves in the range 45–54 °C showcase the modified LCST and combined temperature response of PNIPAm and crosslinked gelatin in the gel system. The formation of a crosslinked network dropped the pore size of the gels to 4–5 μm, and the system demonstrated adhesion to various substrates. The developed biocompatible self-healing adhesive gels can be used for various applications, including tissue engineering, drug delivery systems, wound healing materials, and soft robotics. Moreover, the photoluminescence characteristic can facilitate the monitoring of localized wounds.

Data availability

Data will be made available on request.

Conflicts of interest

There are no conflicts of interest to declare.

Acknowledgements

Author P. A. Parvathy is grateful to Department of Science and Technology, Government of India for the Inspire fellowship grant (IF190279). Dr Sriparna De would like to acknowledge the SEED Research grant, Brainware University (BWU/PRJ/SMG/22-23/001) for providing research support and facilities.

References

1 P. Bertsch, M. Diba, D. J. Mooney and S. C. G. Leeuwenburgh, Self-Healing Injectable Hydrogels for Tissue Regeneration, *Chem. Rev.*, 2023, **123**(2), 834–873, DOI: 10.1021/acs.chemrev.2c00179.

2 S. Nejati and L. Mongeau, Injectable, Pore-Forming, Self-Healing, and Adhesive Hyaluronan Hydrogels for Soft Tissue Engineering Applications, *Sci. Rep.*, 2023, **13**(1), 1–12, DOI: 10.1038/s41598-023-41468-9.

3 J. Chen and X. Zou, Self-Assemble Peptide Biomaterials and Their Biomedical Applications, *Bioact. Mater.*, 2019, **4**, 120–131, DOI: 10.1016/j.bioactmat.2019.01.002.

4 J. Xu, Y. Liu and S. Hsu, Hydrogels Based on Schi Ff Base Linkages For, *Molecules*, 2019, **24**(3005), 1–21.

5 L. Xu, R. Qin, J. Zhang, J. Liu, S. Liu, F. Li, A. Gong, Q. Hanliang, F. Du and M. Zhang, Mussel-Inspiredin Situfabrication of a Photothermal Composite Hydrogel for

MR-Guided Localized Tumor Ablation, *RSC Adv.*, 2021, **11**(32), 19461–19469, DOI: 10.1039/d1ra00903f.

6 Y. Cheng, H. Zhang, H. Wei and C. Y. Yu, Injectable Hydrogels as Emerging Drug-Delivery Platforms for Tumor Therapy, *Biomater. Sci.*, 2024, **12**(5), 1151–1170, DOI: 10.1039/d3bm01840g.

7 A. Atwal, T. P. Dale, M. Snow, N. R. Forsyth and P. Davoodi, Injectable Hydrogels: An Emerging Therapeutic Strategy for Cartilage Regeneration, *Adv. Colloid Interface Sci.*, 2023, **321**, 103030, DOI: 10.1016/j.cis.2023.103030.

8 M. Diba, H. Wang, T. E. Kodger, S. Parsa and S. C. G. Leeuwenburgh, Highly Elastic and Self-Healing Composite Colloidal Gels, *Adv. Mater.*, 2017, **29**(11), 1604672, DOI: 10.1002/adma.201604672.

9 E. Khare, N. Holten-Andersen and M. J. Buehler, Transition-Metal Coordinate Bonds for Bioinspired Macromolecules with Tunable Mechanical Properties, *Nat. Rev. Mater.*, 2021, **6**(5), 421–436, DOI: 10.1038/s41578-020-00270-z.

10 E. E. Meyer, K. J. Rosenberg and J. Israelachvili, Recent Progress in Understanding Hydrophobic Interactions, *Proc. Natl. Acad. Sci. U. S. A.*, 2006, **103**(43), 15739–15746, DOI: 10.1073/pnas.0606422103.

11 S. Li, J. Yu, M. Zhang, Z. Ma, N. Chen, X. Li, J. Ban, J. Xie, Z. Chen, J. Ma, C. Tian, Y. Qin, J. Wang, W. Gao, L. Long, J. Zhao, X. Hou and X. Yuan, An Intermediate Unit-Mediated, Continuous Structural Inheritance Strategy for the Dilemma between Injectability and Robustness of Hydrogels, *Adv. Funct. Mater.*, 2022, **32**(14), 1–12, DOI: 10.1002/adfm.202110617.

12 M. E. Belowich and J. F. Stoddart, Dynamic Imine Chemistry, *Chem. Soc. Rev.*, 2012, **41**(6), 2003–2024, DOI: 10.1039/c2cs15305j.

13 B. Lewis, J. M. Dennis and K. R. Shull, Effects of Dynamic Disulfide Bonds on Mechanical Behavior in Glassy Epoxy Thermosets, *ACS Appl. Polym. Mater.*, 2023, **5**(4), 2583–2595, DOI: 10.1021/acsapm.2c02194.

14 S. M. Morozova, Recent Advances in Hydrogels via Diels–Alder Crosslinking: Design and Applications, *Gels*, 2001, **37**(7), 161.

15 L. Terriac, J. J. Helesbeux, Y. Maugars, J. Guicheux, M. W. Tibbitt and V. Delplace, Boronate Ester Hydrogels for Biomedical Applications: Challenges and Opportunities, *Chem. Mater.*, 2024, **36**(14), 6674–6695, DOI: 10.1021/acs.chemmater.4c00507.

16 Y. Liu, Y. Liu, Q. Wang, Y. Han, H. Chen and Y. Tan, Doubly Dynamic Hydrogel Formed by Combining Boronate Ester and Acylhydrazone Bonds, *Polymers*, 2020, **12**(2), 1–15, DOI: 10.3390/polym12020487.

17 L. Li, X. Peng, D. Zhu, J. Zhang and P. Xiao, Recent Progress in Polymers with Dynamic Covalent Bonds, *Macromol. Chem. Phys.*, 2023, **224**(20), 1–25, DOI: 10.1002/macp.202300224.

18 T. Huang, W. Zhang, S. Yang, L. Wang and G. Yu, Imine-Linked Covalent Organic Frameworks: Recent Advances in Design, Synthesis, and Application, *SmartMat*, 2024, 1–40, DOI: 10.1002/smm2.1309.

19 X. Wang, H. J. Zhang, Y. Yang, Y. Chen, X. Zhu and X. You, Biopolymer-Based Self-Healing Hydrogels: A Short Review, *Giant*, 2023, **16**, 100188, DOI: 10.1016/j.giant.2023.100188.

20 R. Bui and M. A. Brook, Dynamic Covalent Schiff-Base Silicone Polymers and Elastomers, *Polymer*, 2019, **160**, 282–290, DOI: 10.1016/j.polymer.2018.11.043.

21 Z. Liu, Y. Tang, Y. Chen, Z. Lu and Z. Rui, Dynamic Covalent Adhesives and Their Applications: Current Progress and Future Perspectives, *Chem. Eng. J.*, 2024, **497**, 154710, DOI: 10.1016/j.cej.2024.154710.

22 Q. Wang, Y. Zhang, Y. Ma, M. Wang and G. Pan, Nano-Crosslinked Dynamic Hydrogels for Biomedical Applications, *Mater. Today Bio*, 2023, **20**, 100640, DOI: 10.1016/j.mtbio.2023.100640.

23 M. Wu, J. Chen, W. Huang, B. Yan, Q. Peng, J. Liu, L. Chen and H. Zeng, Injectable and Self-Healing Nanocomposite Hydrogels with Ultrasensitive PH-Responsiveness and Tunable Mechanical Properties: Implications for Controlled Drug Delivery, *Biomacromolecules*, 2020, **21**(6), 2409–2420, DOI: 10.1021/acs.biomac.0c00347.

24 Y. H. Yeo and W. H. Park, Dual-Crosslinked, Self-Healing and Thermo-Responsive Methylcellulose/Chitosan Oligomer Copolymer Hydrogels, *Carbohydr. Polym.*, 2021, **258**, 117705, DOI: 10.1016/j.carbpol.2021.117705.

25 F. Gang, H. Yan, C. Ma, L. Jiang, Y. Gu, Z. Liu, L. Zhao, X. Wang, J. Zhang and X. Sun, Robust Magnetic Double-Network Hydrogels with Self-Healing, MR Imaging, Cytocompatibility and 3D Printability, *Chem. Commun.*, 2019, **55**(66), 9801–9804, DOI: 10.1039/c9cc04241e.

26 R. Xing, K. Liu, T. Jiao, N. Zhang, K. Ma, R. Zhang, Q. Zou, G. Ma and X. Yan, An Injectable Self-Assembling Collagen-Gold Hybrid Hydrogel for Combinatorial Antitumor Photothermal/Photodynamic Therapy, *Adv. Mater.*, 2016, **28**(19), 3669–3676, DOI: 10.1002/adma.201600284.

27 Z. Dou, H. Tang, K. Chen, D. Li, Q. Ying, Z. Mu, C. An, F. Shao, Y. Zhang, Y. Zhang, H. Bai, G. Zheng, L. Zhang, T. Chen and H. Wang, Highly Elastic and Self-Healing Nanostructured Gelatin/Clay Colloidal Gels with Osteogenic Capacity for Minimally Invasive and Customized Bone Regeneration, *Biofabrication*, 2023, **15**(2), 025001, DOI: 10.1088/1758-5090/acab36.

28 J. Liu, G. Song, C. He and H. Wang, Self-Healing in Tough Graphene Oxide Composite Hydrogels, *Macromol. Rapid Commun.*, 2013, **34**(12), 1002–1007, DOI: 10.1002/marc.201300242.

29 Y. Miao, Y. Chen, J. Luo, X. Liu, Q. Yang, X. Shi and Y. Wang, Black Phosphorus Nanosheets-Enabled DNA Hydrogel Integrating 3D-Printed Scaffold for Promoting Vascularized Bone Regeneration, *Bioact. Mater.*, 2023, **21**, 97–109, DOI: 10.1016/j.bioactmat.2022.08.005.

30 W. Ma, W. Cao, T. Lu, Z. Jiang, R. Xiong, S. K. Samal and C. Huang, Healable, Adhesive, and Conductive Nanocomposite Hydrogels with Ultrastretchability for Flexible Sensors, *ACS Appl. Mater. Interfaces*, 2021, **13**(48), 58048–58058, DOI: 10.1021/acsami.1c20271.

31 E. Pocurull, N. Fontanals, M. Calull and C. Aguilar, Natural and Synthetic Polymers for Biomedical and Environmental Applications, *Polymers*, 2019, 591–641, DOI: 10.1016/B978-0-12-816911-7.00020-7.

32 L. Li, F. Yu, L. Zheng, R. Wang, W. Yan, Z. Wang, J. Xu, J. Wu, D. Shi, L. Zhu, X. Wang and Q. Jiang, Natural Hydrogels for Cartilage Regeneration: Modification, Preparation and Application, *J. Orthop. Transl.*, 2019, **17**(2), 26–41, DOI: 10.1016/j.jot.2018.09.003.

33 T. Kopač, Mathematical Model for Characterization of Temperature-Responsive Polymers: A Study on the Rheological Behavior of Gelatin and Poly (N-Isopropylacrylamide), *Polym. Test.*, 2024, 133, DOI: 10.1016/j.polymertesting.2024.108402.

34 M. Le, W. Huang, K. F. Chen, C. Lin, L. Cai, H. Zhang and Y. G. Jia, Upper Critical Solution Temperature Polymeric Drug Carriers, *Chem. Eng. J.*, 2022, **432**, 134354, DOI: 10.1016/j.cej.2021.134354.

35 Y. H. Cheng, E. Chavez, K. L. Tsai, K. C. Yang, W. T. Kuo, Y. P. Yang, S. H. Chiou and F. H. Lin, *Effects of Thermosensitive Chitosan-Gelatin Based Hydrogel Containing Glutathione on Cisd2-Deficient Chondrocytes under Oxidative Stress*, Elsevier Ltd., 2017, vol. 173. DOI: 10.1016/j.carbpol.2017.05.069.

36 Y. H. Cheng, Y. C. Ko, Y. F. Chang, S. H. Huang and C. J. L. Liu, Thermosensitive Chitosan-Gelatin-Based Hydrogel Containing Curcumin-Loaded Nanoparticles and Latanoprost as a Dual-Drug Delivery System for Glaucoma Treatment, *Exp. Eye Res.*, 2019, **179**, 179–187, DOI: 10.1016/j.exer.2018.11.017.

37 R. Andreazza, A. Morales, S. Pieniz and J. Labidi, Gelatin-Based Hydrogels: Potential Biomaterials for Remediation, *Polymers*, 2023, **15**(4), 1–12, DOI: 10.3390/polym15041026.

38 S. Chatterjee and P. C. L. Hui, Review of Applications and Future Prospects of Stimuli-Responsive Hydrogel Based on Thermo-Responsive Biopolymers in Drug Delivery Systems, *Polymers*, 2021, **13**(13), 2086, DOI: 10.3390/polym13132086.

39 Y. Li, J. Luo, G. Xie, D. Zhu, C. Zhao, X. Zhang, M. Liu, Y. Wu, Y. Guo and W. Yu, Recent Progress on Regulating the LCST of PNIPAM-Based Thermochromic Materials, *ACS Appl. Polym. Mater.*, 2024, **7**, 1–11, DOI: 10.1021/acsapm.4c03406.

40 N. A. Shaibie, N. A. Ramli, N. D. F. Mohammad Faizal, T. Srichana and M. C. I. Mohd Amin, Poly (N-Isopropylacrylamide)-Based Polymers: Recent Overview for the Development of Temperature-Responsive Drug Delivery and Biomedical Applications, *Macromol. Chem. Phys.*, 2023, **224**(20), 1–12, DOI: 10.1002/macp.202300157.

41 S. Dolui, B. Sahu, S. A. Mohammad and S. Banerjee, Multi-Stimuli Responsive Sequence Defined Multi-Arm Star Diblock Copolymers for Controlled Drug Release, *JACS Au*, 2023, **3**(8), 2117–2122, DOI: 10.1021/jacsau.3c00339.

42 I. Sanzari, E. Buratti, R. Huang, C. G. Tusan, F. Dinelli, N. D. Evans, T. Prodromakis and M. Bertoldo, Poly (N-Isopropylacrylamide) Based Thin Microgel Films for Use in Cell Culture Applications, *Sci. Rep.*, 2020, **10**(1), 1–14.

43 S. A. Mohammad, S. Dolui, D. Kumar, M. M. Alam and S. Banerjee, Anisotropic and Self-Healing Copolymer with Multiresponsive Capability via Recyclable Alloy-Mediated RDRP, *Macromol. Rapid Commun.*, 2021, **42**(12), 1–7, DOI: 10.1002/marc.202100096.

44 V. Bütün, S. Liu, J. V. M. Weaver, X. Bories-Azeau, Y. Cai and S. P. Armes, A Brief Review of "schizophrenic" Block Copolymers, *React. Funct. Polym.*, 2006, **66**(1), 157–165, DOI: 10.1016/j.reactfunctpolym.2005.07.021.

45 Y. Nan, C. Zhao, G. Beaudoin and X. X. Zhu, Synergistic Approaches in the Design and Applications of UCST Polymers, *Macromol. Rapid Commun.*, 2023, **44**(23), 1–16, DOI: 10.1002/marc.202300261.

46 M. Aggarwal, H. Panigrahi, D. K. Kotnees and P. Das, Multifunctional Self-Healing Carbon Dot-Gelatin Bioadhesive: Improved Tissue Adhesion with Simultaneous Drug Delivery, Optical Tracking, and Photoactivated Sterilization, *Biomacromolecules*, 2024, **25**(5), 3178–3189, DOI: 10.1021/acs.biomac.4c00313.

47 W. Sun, J. Zhu, Z. Cui, C. Zhou, S. Guo, W. Li and J. Qin, Self-Healing Hydrogel Prepared from Gallic Acid Coupled P(NIPAM-Co-AH) and Oxidized Sodium Alginate for Diabetic Wound Repairing, *React. Funct. Polym.*, 2024, **201**, 105951, DOI: 10.1016/j.reactfunctpolym.2024.105951.

48 T. Khodaei, J. Nourmohammadi, A. Ghaee and Z. Khodaii, An Antibacterial and Self-Healing Hydrogel from Aldehyde-Carrageenan for Wound Healing Applications, *Carbohydr. Polym.*, 2023, **302**, 120371, DOI: 10.1016/j.carbpol.2022.120371.

49 J. W. Guo, C. F. Wang, J. Y. Lai, C. H. Lu and J. K. Chen, Poly(N-Isopropylacrylamide)-Gelatin Hydrogel Membranes with Thermo-Tunable Pores for Water Flux Gating and Protein Separation, *J. Membr. Sci.*, 2021, **618**, 118732, DOI: 10.1016/j.memsci.2020.118732.

50 P. A. Parvathy, S. De, M. Singh, G. Manik and S. K. Sahoo, RAFT Polymerization Assisted P (NIPAm- Co -AAc) -AEMR Integrated PVA Hydrogels: Dual Responsive Features, Texture Analysis, and Cytotoxicity Studies, *React. Funct. Polym.*, 2024, **205**, 106052, DOI: 10.1016/j.reactfunctpolym.2024.106052.

51 L. Raju, A. R. Stesho Crystalin Lazuli, N. K. Udaya Prakash and E. Rajkumar, Chitosan-Terephthaldehyde Hydrogels – Effect of Concentration of Cross-Linker on Structural, Swelling, Thermal and Antimicrobial Properties, *Materialia*, 2021, **16**, 101082, DOI: 10.1016/j.mtla.2021.101082.

52 S. Kumar and J. Koh, Physiochemical and Optical Study of Chitosan-Terephthaldehyde Derivative for Biomedical Applications, *Int. J. Biol. Macromol.*, 2012, **51**(5), 1167–1172, DOI: 10.1016/j.ijbiomac.2012.09.001.

53 S. Farris, J. Song and Q. Huang, Alternative Reaction Mechanism for the Cross-Linking of Gelatin with Glutaraldehyde, *J. Agric. Food Chem.*, 2010, **58**(2), 998–1003, DOI: 10.1021/jf9031603.

54 H. W. Yang, A. W. Lee, C. H. Huang and J. K. Chen, Characterization of Poly(N-Isopropylacrylamide)-Nucleobase Supramolecular Complexes Featuring Bio-

Multiple Hydrogen Bonds, *Soft Matter*, 2014, **10**(41), 8330–8340, DOI: 10.1039/c4sm01496k.

55 J. Joy, A. Gupta, S. Jahnavi, R. S. Verma, A. R. Ray and B. Gupta, Understanding the in Situ Crosslinked Gelatin Hydrogel, *Polym. Int.*, 2016, **65**(2), 181–191, DOI: 10.1002/pi.5042.

56 Y. Qian, K. Zhang and F. Chen, *Cross-Linking of Gelatin and Chitosan Complex Nanofibers for Tissue-Engineering Scaffolds*, 2012, pp. 1099–1113.

57 Y. Dong, H. Chen, P. Qiao and Z. Liu, Development and Properties of Fish Gelatin/Oxidized Starch Double Network Film Catalyzed by Thermal Treatment and Schiff' Base Reaction, *Polymers*, 2019, **11**(12), 1–14, DOI: 10.3390/polym11122065.

58 P. Promdontree, A. Ounkaew, Y. Yao, H. Zeng, R. Narain and S. Ummartyotin, Temperature-Responsive Injectable Composite Hydrogels Based on Poly (N-Isopropylacrylamide), Chitosan, and Hemp-Derived Cellulose Nanocrystals, *Polymers*, 2024, **16**(21), 2984, DOI: 10.3390/polym16212984.

59 A. Trubetskaya, J. Leppiniemi, S. Lipponen, S. Lombardo, W. Thielemans, T. Maloney, T. Pääkkönen, K. K. Kesari, J. Ruokolainen, V. P. Hytönen and E. Kontturi, Thermoresponsive and Biocompatible Poly (N-Isopropylacrylamide)-Cellulose Nanocrystals Hydrogel for Cell Growth, *Mater. Adv.*, 2023, **5**(2), 570–583, DOI: 10.1039/d3ma00495c.

60 M. Qi, L. Zheng, C. Li, Y. Xiao, J. Liu, S. Wu and B. Zhang, The Yellowing Mechanism of Polyesteramide Based on Poly (Ethylene Terephthalate) and Polyamide 6, *J. Appl. Polym. Sci.*, 2021, **138**(10), 1–10, DOI: 10.1002/app.49986.

61 P. R. Chen, P. L. Kang, W. Y. Su, F. H. Lin and M. H. Chen, The Evaluation of Thermal Properties and in Vitro Test of Carbodiimide or Glutaraldehyde Cross-Linked Gelatin for PC 12 Cells Culture, *Biomed. Eng.*, 2005, **17**(2), 101–107, DOI: 10.4015/S1016237205000160.

62 P. A. Parvathy, S. De, M. Singh, G. Manik and S. K. Sahoo, RAFT Polymerization Assisted P(NIPAm-Co-AAc)-AEMR Integrated PVA Hydrogels: Dual Responsive Features, Texture Analysis, and Cytotoxicity Studies, *React. Funct. Polym.*, 2024, **205**, 106052, DOI: 10.1016/j.reactfunctpolym.2024.106052.

63 S. De, A. Ghosh, D. Mandal, K. Sarkar, A. P. Samanta, M. Basak, A. Saha, D. Bhattacharya, S. Nandi, J. Sarkar, M. Mandal, K. Acharya, P. Ghosh and D. Chattopadhyay, Lysine-Mediated Yttrium Oxide Nanoparticle–Incorporated Nanofibrous Scaffolds with Tunable Cell Adhesion, Proliferation, and Antimicrobial Potency for In Vitro Wound-Healing Applications, *ACS Appl. Bio Mater.*, 2024, 6414–6429, DOI: 10.1021/acsabm.4c00551.

64 Q. Weng, J. Yi, X. Chen, D. Luo, Y. Wang, W. Sun, J. Kang and Z. Han, Controllable Synthesis and Biological Application of Schiff Bases from d -Glucosamine and Terephthalaldehyde, *ACS Omega*, 2020, **5**(38), 24864–24870, DOI: 10.1021/acsomega.0c03591.